 ICCES, vol.1, no.1, pp.29-34, 2007

Automated Segmentation of Atherosclerotic Plaque Using Bayes Classifier for Multi-Contrast *In Vivo* and *Ex Vivo* MR Images

Xueying Huang[1], Chun Yang[2], Jie Zheng[3], Pamela K. Woodard[3] and Dalin Tang[1]

Summary

Atherosclerotic plaques may rupture without warning and cause acute cardiovascular syndromes such as heart attack and stroke. Accurate identification of plaque components will improve the accuracy and reliability of computational models. In this article, we present a segmentation method using a cluster analysis technique to quantify and classify plaque components from magnetic resonance images (MRI). 3D *in vivo* and *ex vivo* multi-contrast (T1-, proton density-, and T2-weighted) MR Images were acquired from a patient of cardiovascular disease. Normal distribution Bayes classifier was performed on *ex vivo* and *in vivo* MR Images respectively. The resulting segmentation obtained from cluster analysis showed very good agreement with histological data. 3D visualization of the plaque was presented. Combination of *in vivo* and *ex vivo* MRI data enabled us to quantify the shrinkage between the *ex vivo* plaque sample and its *in vivo* state. For this patient, the average shrinkage is 9.14% at cross section and 33.33% in axial direction. This information is essential to determining proper initial stress/strain conditions for computational plaque models.

Introduction

Cardiovascular disease (CVD) is the No. 1 killer in the western world [1]. Many critical cardiovascular events such as stroke and heart attack are related to rupture of a vulnerable atherosclerotic plaque in diseased arteries. It is of great importance that non-invasive methods be developed to assess and identify vulnerable atherosclerotic plaques and predict possible plaque rupture before it actually happens. MRI-based computational models can be used to perform mechanical analysis non-invasively to identify critical flow and stress/strain conditions which may be related to possible plaque rupture [4-5]. Plaque morphology is the most basic element needed to construct computational models.

High resolution MRI is capable of quantify plaque morphology and plaque components. Most of these are generally based on a manual extraction of numerous contours. Automated segmentation procedure would permit combination of multi-contrast weighting MR Image. It was hypothesized that multi-contrast MR images could enhance the differentiation of various tissue components based on their signal intensities in different MR Weightings. In this paper, an automated multi-contrast

[1]Mathematics Department, Worcester Polytechnic Institute, Worcester, MA 01609, USA
[2]Mathematics Department, Beijing Normal University, Beijing, China
[3]Mallinkcrodt Institute of Radiology, Washington University, St. Louis, MO 63110, USA

plaque segmentation method using Bayesian Classifier with Normal distribution probability is introduced. Results from *in vivo* and *ex vivo* MRI of a patient were obtained and validated by histological data. Artery shrinkage in cross-section and axial direction were quantified by comparing *in vivo* and *ex vivo* MRI data.

Materials and Method

3D *in vivo*, *ex vivo* MRI, and histological images of a patient were provided by Dr. Zheng's group using protocol approved by Washington University Institutional Review Board with informed consent obtained. The *in vivo* imaging data set included multi-contrast weighting images with T1-, T2- and proton density (PD) weightings. Each contrast weighting session consists of 14 2D slices with high resolution (200×200 μm^2, slice thickness=3mm). The *ex vivo* imaging data set included T1-, T2-, gradient-echo (GRE) and proton density(PD) weighted MR Images. Each contrast weighting session has 30 2D slices with high resolution (109×109 μm^2, slice thickness=1mm).

The intensity of each image was not uniform due to the effects of coil inhomogeneity and was adjusted (see Fig. 1). A 14mm$\times$14mm region was selected as the region of interest (ROI). The contrast of the images was increased by linear transformation. The effect of this pre-processing is shown by Fig. 1.

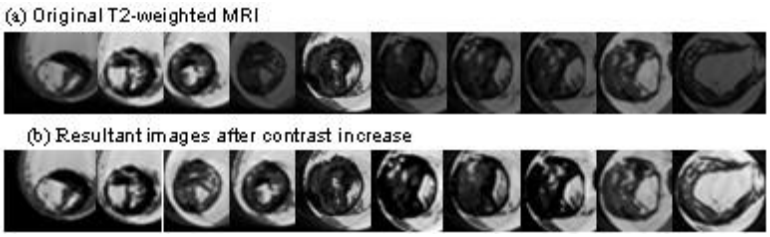

Figure 1: Pre-Processing results of selected slices from all 32 slices of *ex vivo* MR Images: (a) original T2-weighted MR images; (b) resultant images after contrast increase.

From *ex vivo* MRI slices with matching histological slices, slices 14 and 26 were selected to generate the training set for segmentation. Images of those two slices were manually segmented based on registered histological results and relative intensity. A total of 573 pixels (each pixel contains 4 densities representing all 4 different contrast weightings) were selected randomly for study. From these segmentation results, each location was determined to belong to one of the 4 issue types including lipid (denoted as Z_1), normal issue (denoted as Z_2), calcification (denoted as Z_3) and others (including lumen or outer issue, denoted as Z_4). The training set was used to generate the probability function which was used to determine the probability of tissue type for each pixel.

The most important part of the segmentation algorithm is to determine the prob-

abilities of each pixel. These probabilities represent the likelihood that the tissue at the location of the pixel is lipid, calcification, normal issue or others. We determine those probabilities base on all the intensity of each weighting MR Images. The intensity vector$\vec{I} = (I_1, I_2, I_3, I_4)$ is used to represent the intensity of the pixel in one of the contrast weighting MR Images and Z_i, i=1, 2, 3, 4, corresponds to the label of the issue. We used$P(Z_i|\vec{I})$to represent the probability of $\vec{I}$ belongs to Z_i. Assume that I_i is conditional independent of $I_j, (i \neq j)$, that is, the intensity of one of the contrast weighting MRI do not depend on other contrast weighting MRI. This assumption allows us to calculate the posterior probability using naive-Bayes decision theory [2],

$$P(Z_i|\vec{I}) = \frac{P(Z_i)P(\vec{I}|Z_i)}{\sum_{i=1}^{4} P(Z_i)P(I_1|Z_i)P(I_2|Z_i)P(I_3|Z_i)P(I_4|Z_i)} \quad (1)$$

The prior probability $P(Z_i)$ was estimated by the frequency of each of the 4 tissue from the training set. Assume that the conditional probability density function (pdf) is a normal distribution, denoted by $P(I_j|Z_i) \sim N(\mu_{ji}, \sigma_{ji})$, where$\mu_{ji}and\sigma_{ji}$is the unbiased estimation of mean value and standard deviation respectively of ith issue type for jth contrast weighting images.

Maximum classifier was used to determine which issue type the pixel belongs to. Fig. 2 gives the flowchart of our maximum decision probability functional classifier. Where$\vec{I}$ is multi-contrast weighting MR Images transformed by preprocessing,$g_i(\vec{I})$ is the decision function pdf $P(Z_i|\vec{I})$. If $g_i(\vec{I})$ is the maximum value, then pixel $\vec{I}$ belongs to Z_i and be labeled i.

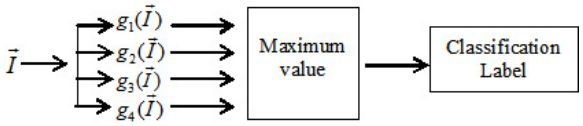

Figure 2: Flowchart of maximum decision probability functional classifier.

Result

Fig 3 shows the results of segmentation of slice 24 of *ex vivo* MR images based on probabilities. Fig 3(a) gives the results of classifier with lipid in red, calcification in yellow, normal issue in blue, and others (including lumen) in green. Fig 3(b) gives the contour result based on 3(a). Fig 3 (c)-(f) gives the segmentation result on all different contrast weighting MR Images. Fig 3 (g) shows the corresponding histological images, C, L represent calcification, lipid respectively. The results match pathology well. Fig 4 shows contour results of all *ex vivo* MR Images.

Applying the method to *in vivo* MR Images, the contours obtained from S1-S9 is given by Fig 5 (b). *In vivo, ex vivo*, and histologic images were registered to

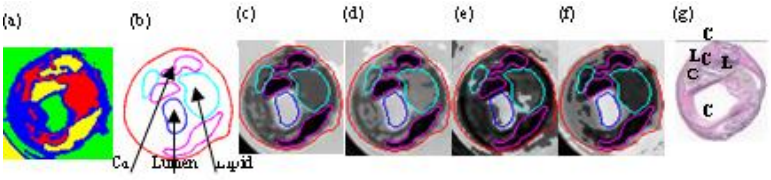

Figure 3: A segmentation example of selected slice using multi-contrast MR Images. (a) Automatic segmentation result of classifier process; (b) Segmented contour result; (c)-(f) give segmentation results on T1, PD, T2, GRE weighting images respectively; (g) shows corresponding histological images. Our contour results show excellent agreement with histopathological data.

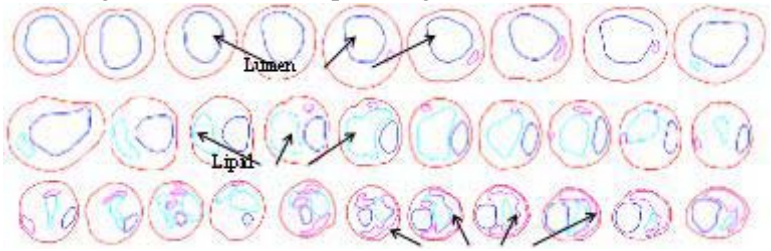

Figure 4: Segmented contour plots of all *ex vivo* MRI slices showing plaque components

match each other. Fig.5 shows the corresponding slices of *ex vivo*, *in vivo* MRI and histology. 3D reconstruction geometry was shown on Fig 6.

Since 1983, when the significance of the zero-stress state of living tissues was recognized, many experiments have been done using 2D artery rings *ex vivo* to quantify the zero-stress state [3]. However, to our knowledge, there has been no report demonstrating the shrinkage (which is by nature 3D) of the artery using *ex vivo* and *in vivo* MR images. Inner circumferences of plaque samples (diameter is not used since plaques are normally very asymmetric) and axial length will be used as the two measures to compute shrinkage rate based on accurate automatic identification of lumen in both *in vivo* and *ex vivo* MRI. Table 1 shows the inner circumferences in same cross section and shrinkage between *ex vivo* and *in vivo* state. The average shrinkage is 9.14%. The inner circumferences did not change too much. Since the slice thickness is 1mm and 3 mm of 3D in *ex vivo* and *in vivo* MRI data set respectively, the length of the specific part of carotid artery is 16mm (S3-S19) at *ex vivo* state and 24 mm (S1-S9) at *in vivo* state. The stretch ratio of length is 33.33%. The shrinkage rate in length of artery is significant. Axial stretch has to be taken into consideration for 3D fluid-structural interaction (FSI) models.

Conclusion

A method to automatically segment *ex vivo* and *in vivo* MRI data set is in-

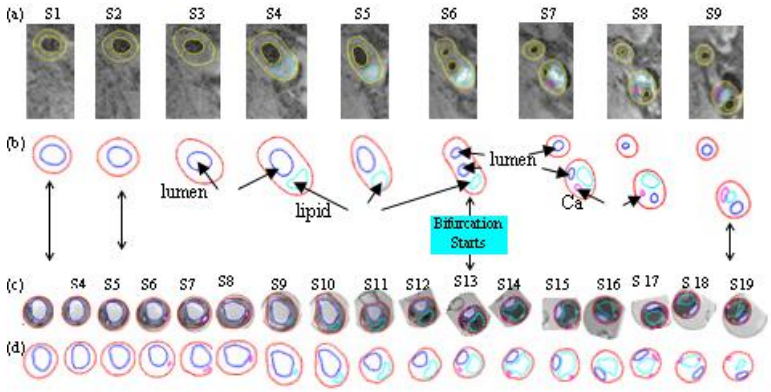

Figure 5: Compare *in vivo*, *ex vivo*, and histological images and the result of segmentations for *in vivo* and *ex vivo* MR Images. (a) Segmentation results on 9 *in vivo* MRI (T1W) slices (S1-S9); (b) Segmented contour plots for (a) showing plaque components; (c) Segmentation results on 17 *ex vivo* MRI (T1) slices (S3-S19); (d) Segmented contour plots for (c) showing plaque components.

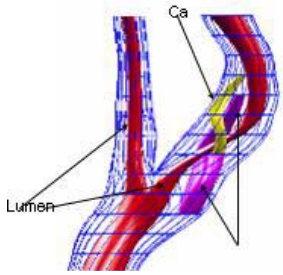

Figure 6: 3D reconstructed geometry of *in vivo* MRI with contour lines.

In vovo	S1	S2	S3	S4	S5	S6	S7	S8	S9
Cin(cm)	1.977	1.908	1.896	2.205	1.876	1.049	0.984	0.947	1.092
Cex(cm)	1.797	1.765	1.892	2.033	1.494	1.066	0.947	0.890	0.774
shrink rate%	9.11	7.50	0.24	7.80	20.37	-1.63	3.84	5.95	29.10

Table 1: Circumferences and shrinkages of lumen measured from segmented contours of *in vivo* and *ex vivo* MRI. Cin and Cex is the circumference of lumen of *in vivo* and *ex vivo* MRI respectively.

troduced. The maximum decision probability functional classifier was applied to multi-contrast weighted MR image processing. Histological images were used to validate the reliability of the segmentation method for multi-contrast weighting *in vivo* and *ex vivo* MR Images. By comparing *in vivo* and *ex vivo* MR images, the shrinkage of artery was calculated. A 9.14% shrinkage in circumferential dimension and 33.33% shrinkage in axial dimension were observed. The combination of *in vivo*, *ex vivo* MRI and Histology may be an important research tool in future studies. Large-scale patient studies are needed to further validate our method and

findings.

Acknowledgement

This research was supported in part by NIH grant NIH/NIBIB, 1 R01 EB004759 and in part by NSF grant DMS-0540684.

References

1. American Heart Association. (2005): *Heart Disease and stroke statistics-2005 Update*.
2. Kuncheva, L.I. (2004): *Combining Pattern Classifiers: Methods and Algorithms*, J Wiley, NJ.
3. Fung, Y.C. (1990): *Biomechanics: Motion, Flow, Stress, and Growth*, Springer, NY
4. Tang, D., Yang, C., Zheng, J., Woodard, P.K., Saffitz, J.E., Sicard, G.A., Pilgram, T.K., Yuan, C. (2005): "Quantifying effects of plaque structure and material properties on stress behaviors in human atherosclerotic plaques using 3D FSI models", *Journal of Biomechanical Engineering*, Vol. 127, pp. 1185-1194.
5. Tang, D., Yang, C., Zheng, J., Woodard P. K., Sicard G. A., Saffitz J. E., and Yuan C.(2004): "3D MRI-Based Multi-Component FSI Models for Atherosclerotic Plaques a 3-D FSI model", *Annals of Biomedical Engineering*, Vol. 32, pp. 947-960.